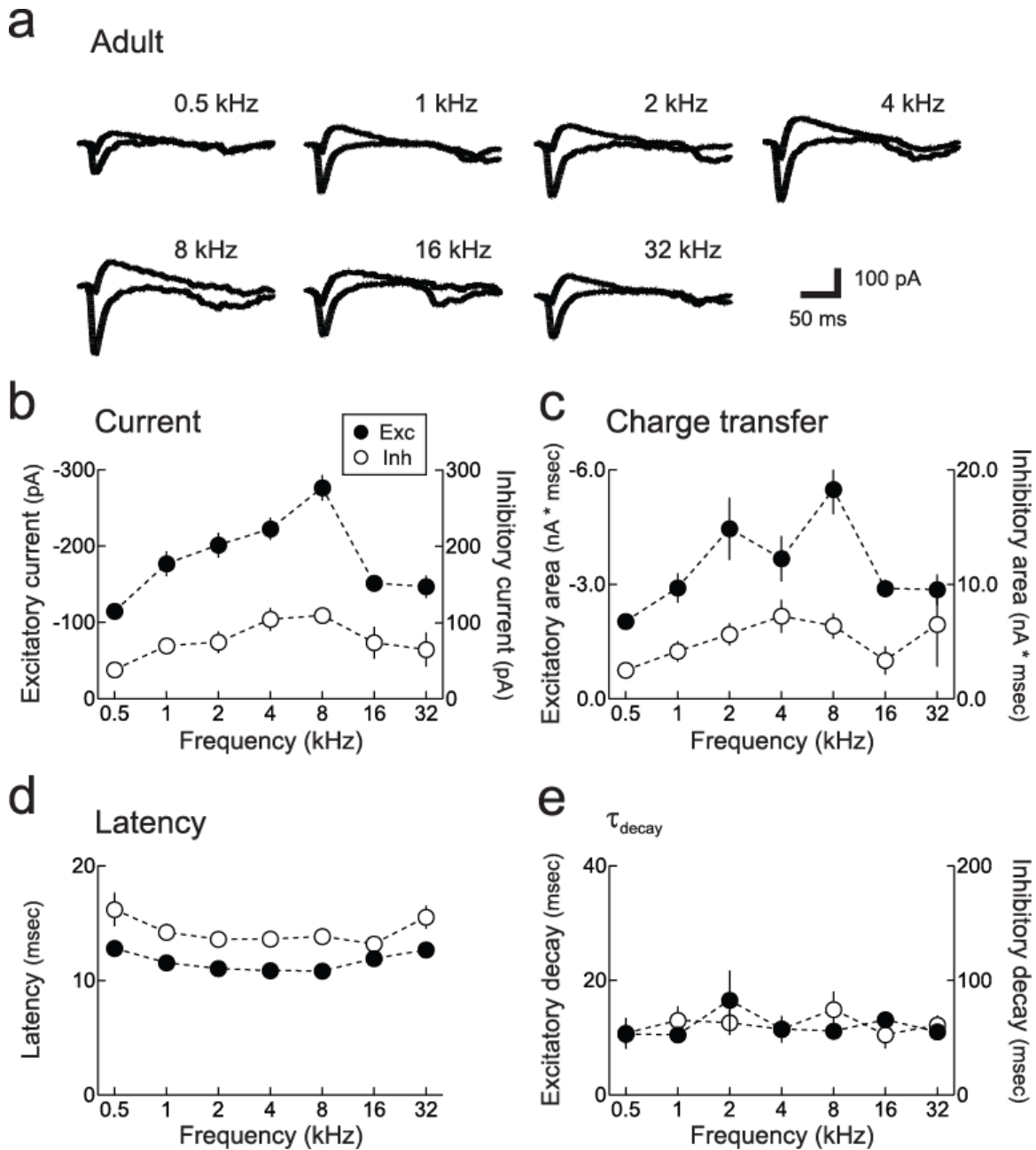


Supplementary Figure 1. Characterization of synaptic tuning curves in young rat AI.

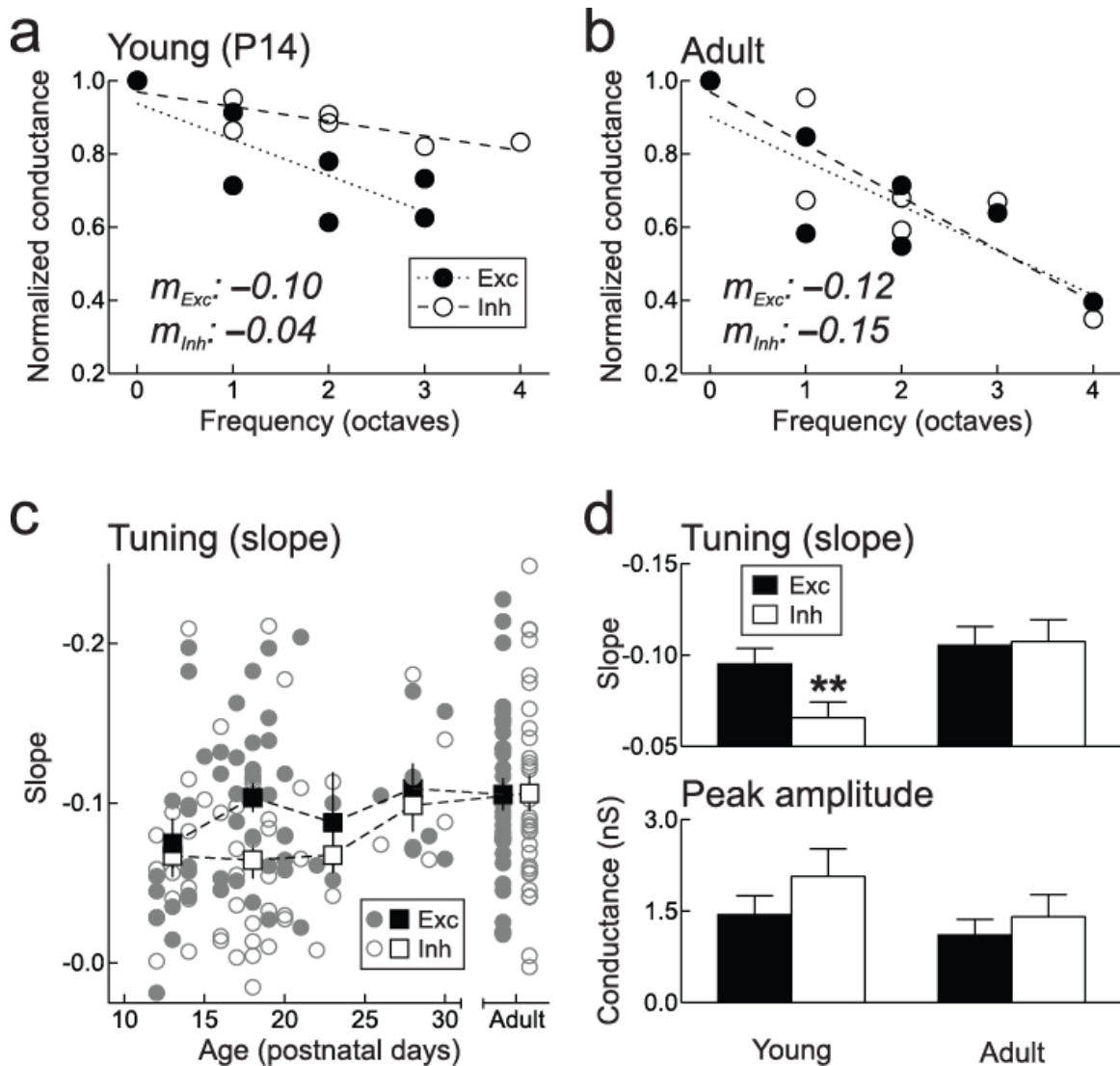
Data are from the P14 neuron shown in Fig. 1a. **a**, Example tone-evoked currents recorded at -70 and 0 mV holding potentials. Scale bar, 50 msec, 100 pA. **b**, Frequency tuning of excitatory and inhibitory currents. Tuning curves for synaptic conductance and current are similar in organization and share the best frequency of excitation (4 kHz). Filled

symbols, excitation; open symbols, inhibition. **c**, Frequency tuning of net charge transfer (synaptic current integrated over 10-200 msec after tone onset). Charge transfer tuning curves are similar to synaptic conductance tuning curves. **d**, Latencies from tone onset to rise of synaptic conductance (10% of peak). Synaptic latency is roughly independent of tone frequency in young animals. **e**, Time constants of synaptic decay (τ_{decay}). τ_{decay} is also approximately independent of tone frequency. Error bars, s.e.m.



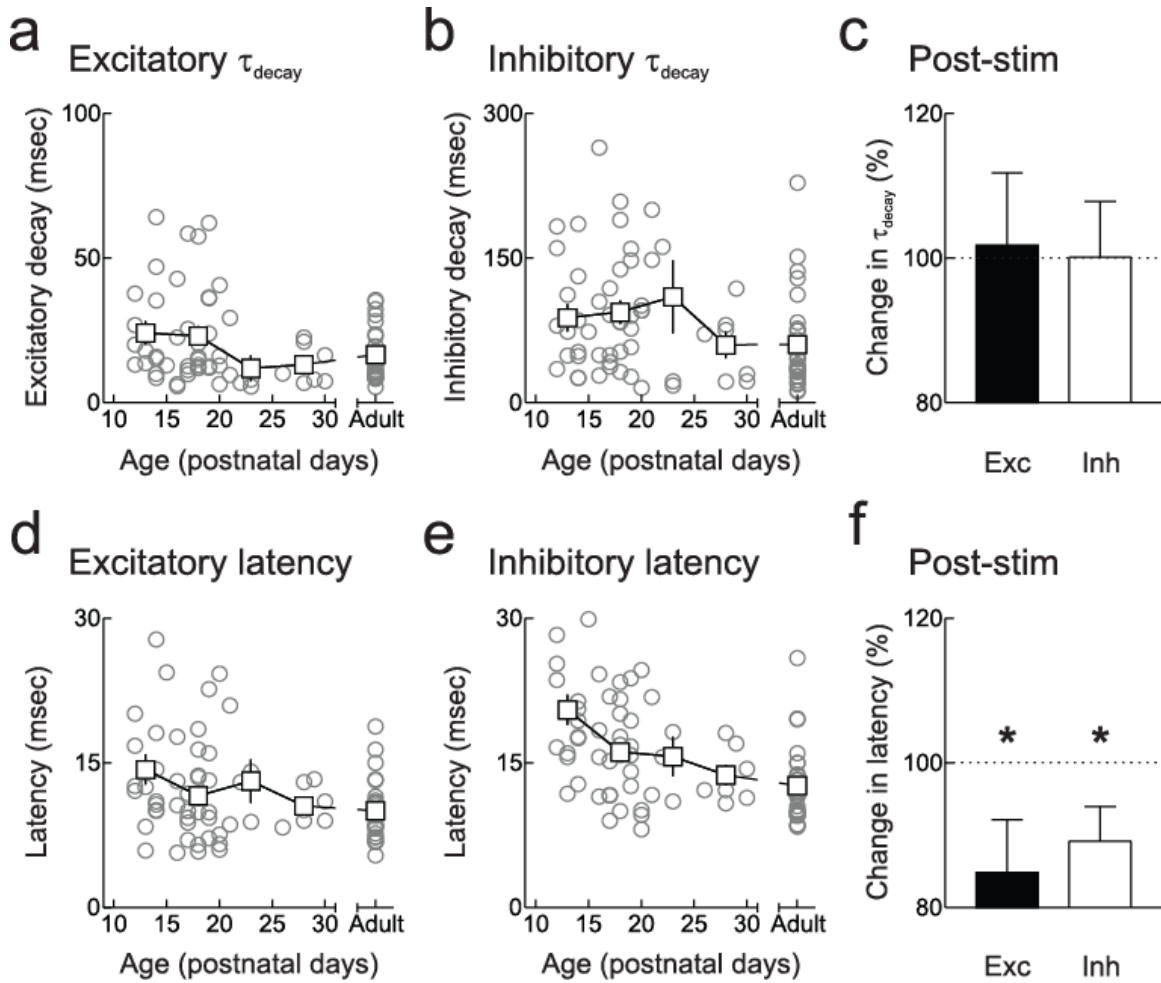
Supplementary Figure 2. Characterization of synaptic tuning curves in adult rat AI. Data are from the neuron shown in Fig. 1b. **a**, Example tone-evoked currents recorded at -70 and 0 mV holding potentials. Scale bar, 50 msec, 100 pA. **b**, Frequency tuning of excitatory and inhibitory currents. Filled symbols, excitation; open symbols, inhibition. **c**, Frequency tuning of net charge transfer. **d**, Latencies from tone onset to rise of

synaptic conductance (10% of peak). Synaptic latency is shortest at best frequency. ϵ ,
 τ_{decay} . τ_{decay} is independent of tone frequency. Error bars, s.e.m.

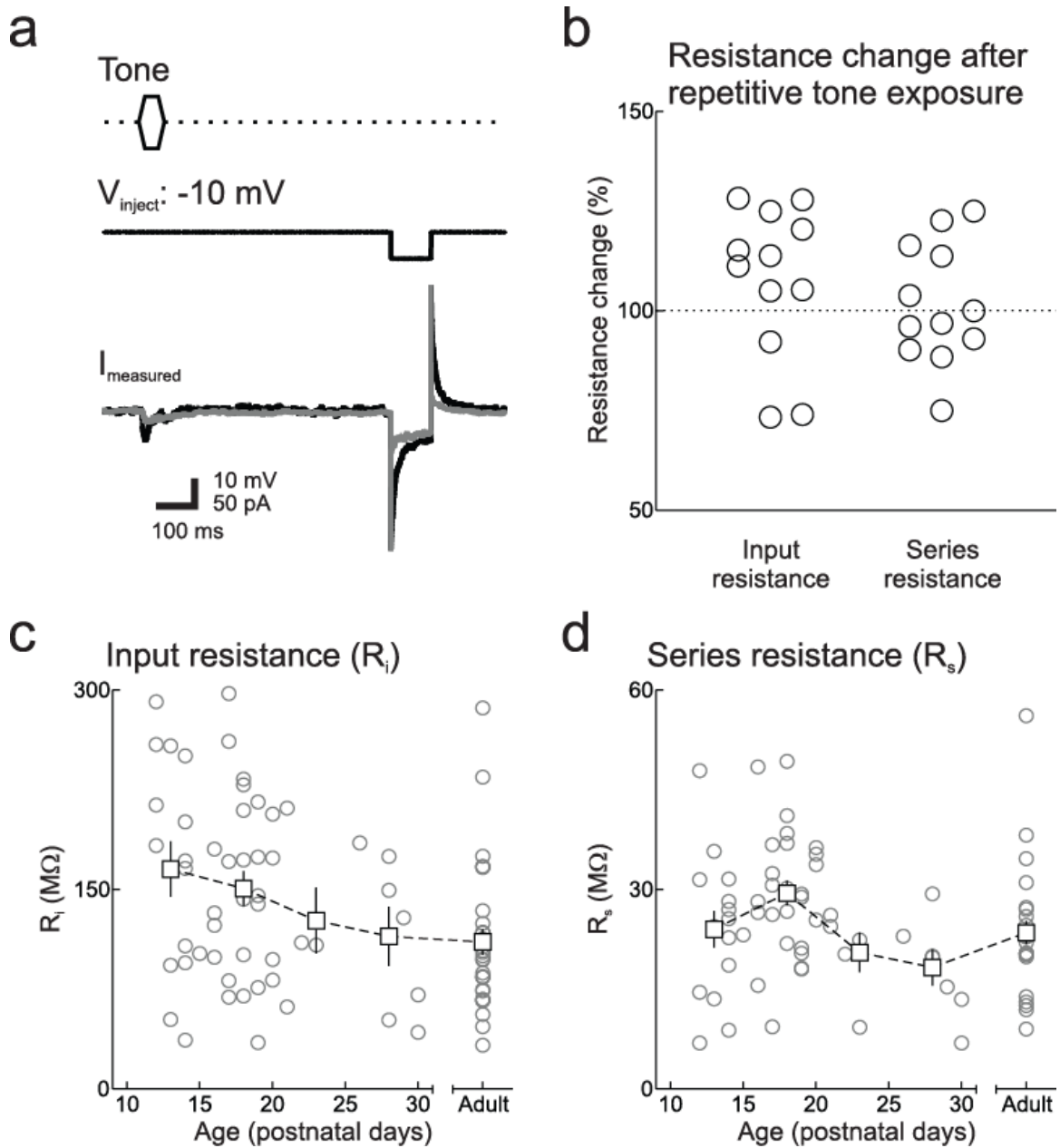


Supplementary Figure 3. Delayed maturation of inhibitory tuning curves as measured by slope. **a**, Excitatory frequency tuning was sharper than inhibitory tuning in early development. Sharpness of tuning was quantified for each cell by normalizing each excitatory (filled symbols) and inhibitory (open symbols) response to the magnitude of conductances evoked by the best frequencies of both excitation and inhibition, respectively, and fitting a line to the normalized tuning curves (excitation, dotted line; inhibition, dashed line). The slope m of the linear fit through the data was used as an

index of tuning sharpness for both excitation (m_{Exc}) and inhibition (m_{Inh}). Data shown here are from the recording in Fig. 1a (P14, m_{Exc} : -0.10 , m_{Inh} : -0.04). **b**, Excitatory and inhibitory frequency tuning were both sharp in adulthood. As in **a**, but data are from the recording in Fig. 1b (adult, m_{Exc} : -0.12 , m_{Inh} : -0.15). **c**, Excitatory frequency tuning sharpened before inhibitory frequency tuning. After the end of the second postnatal week, excitation (filled symbols) and inhibition (open symbols) were weakly tuned (P12-P15, m_{Exc} : -0.07 ± 0.02 , m_{Inh} : -0.07 ± 0.01 , $n=15$, $p>0.4$). Throughout the third week, excitation rapidly sharpened while inhibition was slower to change, with excitation reaching adult levels over this period (P16-P20, m_{Exc} : -0.10 ± 0.01 , m_{Inh} : -0.06 ± 0.01 , $n=26$, $p<0.002$). By the end of the first month, sharpness of synaptic frequency tuning was similar to that measured in adult animals (P26-P30, m_{Exc} : -0.11 ± 0.02 , m_{Inh} : -0.10 ± 0.02 , $n=7$; adults, m_{Exc} : -0.11 ± 0.01 , m_{Inh} : -0.11 ± 0.01 , $n=31$, $p>0.7$ compared to P26-P30). Each cell is represented by a pair of filled and open circles. Squares, summary of results binned over the following age intervals: $\leq P15$, P16-P20, P21-P25, P26-P30, adults; $n=5-31$. **d**, Summary of changes to excitatory and inhibitory tuning over development. Top, mean slope of excitatory and inhibitory tuning in young (P12-P21, m_{Exc} : -0.09 ± 0.01 , m_{Inh} : -0.07 ± 0.01 , $n=43$, $p<0.002$) and adult animals (adults, m_{Exc} : -0.11 ± 0.01 , m_{Inh} : -0.11 ± 0.01 , $n=31$, $p>0.9$). **, $p<0.01$. Bottom, peak amplitude did not change during the AI critical period. Mean amplitude of tone-evoked conductances measured at best frequencies were similar between neurons from young animals (P12-P21, excitation: 1.4 ± 0.3 nS, inhibition: 2.1 ± 0.4 nS, $n=43$) and from adult animals (excitation: 1.1 ± 0.3 nS, $n=31$, $p>0.3$; inhibition: 1.4 ± 0.4 nS, $p>0.2$). Error bars, s.e.m.

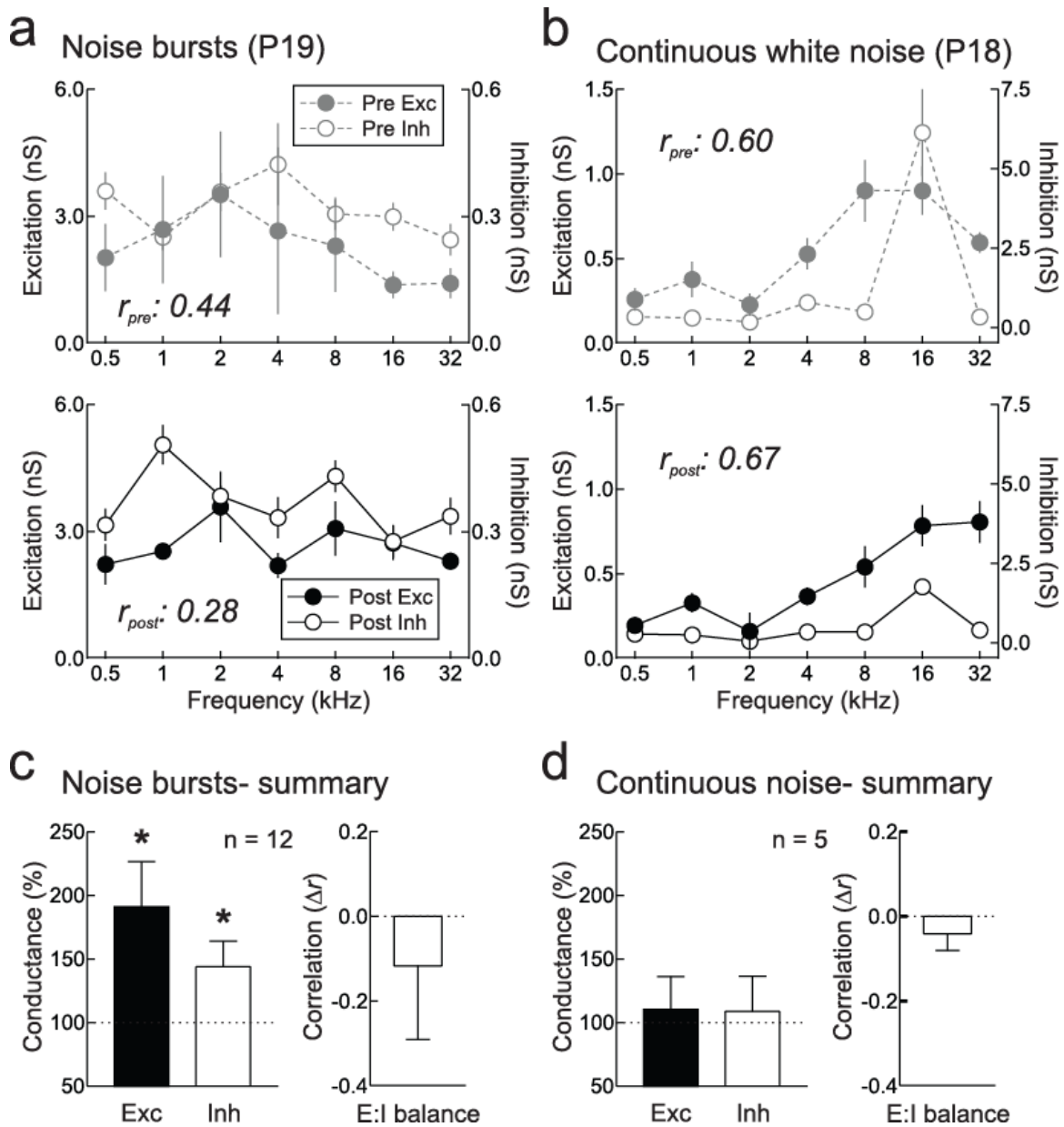


Supplementary Figure 4. Development of synaptic latencies and decay time constants (τ_{decay}). **a**, Excitatory τ_{decay} . **b**, Inhibitory τ_{decay} . **c**, No significant change in excitatory or inhibitory τ_{decay} after patterned stimulation ('post-stim') in P12-P21 animals. **d**, Latency from tone onset to 10% of peak excitatory conductance. **e**, Latency from tone onset to 10% of peak inhibitory conductance. **f**, Excitatory and inhibitory latency decreased after patterned stimulation in P12-P21 animals (change in excitatory response latency of $-15.2 \pm 7.3\%$, change in inhibitory response latency of $-10.8 \pm 4.8\%$, $n=12$, $p < 0.05$). *, $p < 0.05$. Error bars, s.e.m.



Supplementary Figure 5. Resistance measurements over development. **a**, Procedure for measuring input resistance (R_i) and series resistance (R_s). In voltage-clamp, a -10 mV voltage step was applied for 100 msec. Recordings where R_s and R_i changed $<30\%$ 10-20 minutes after pairing (black) compared to 0-10 minutes before pairing (gray) were accepted for analysis. **b**, Relative amount of change in R_s and R_i after patterned

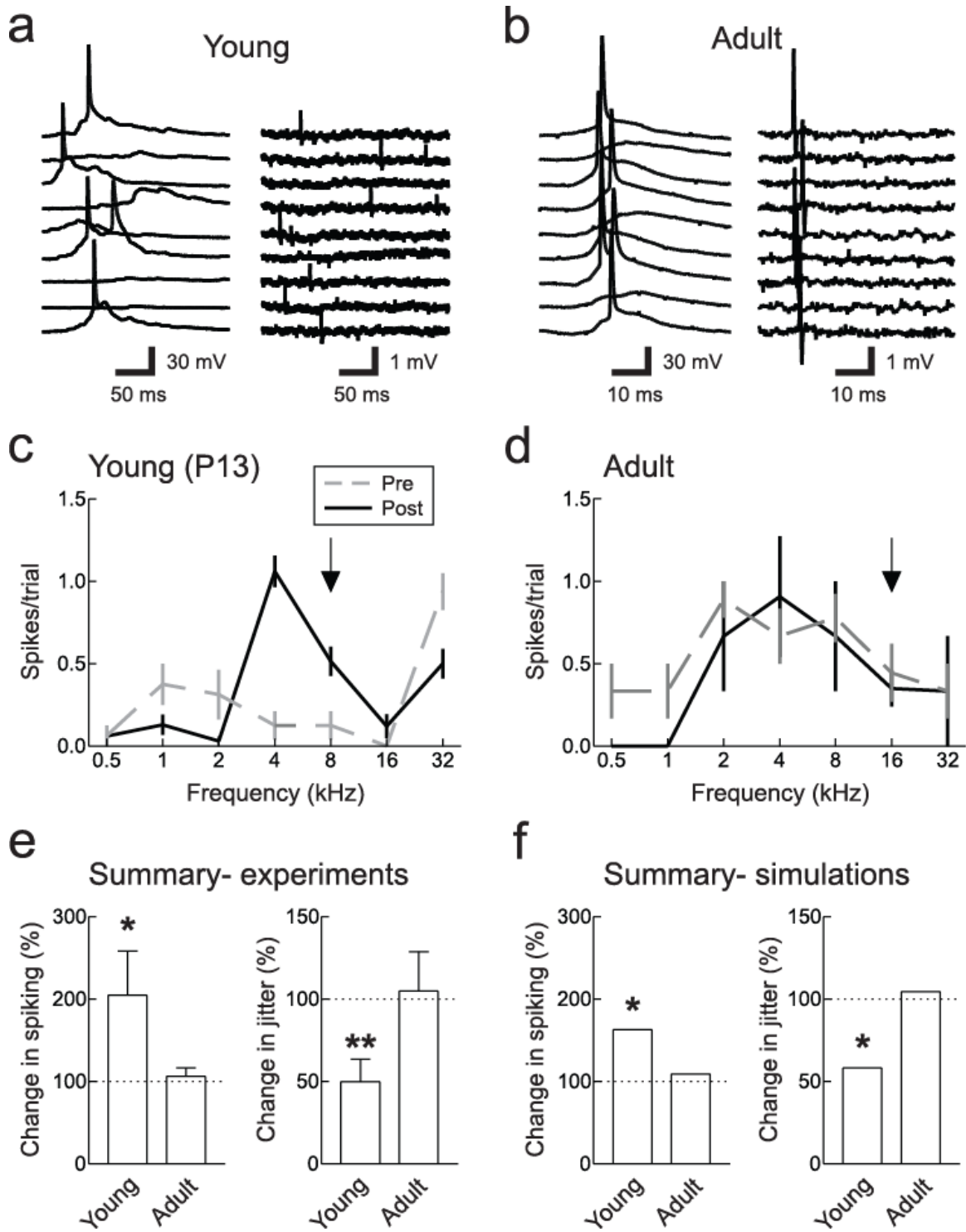
stimulation for those cells included in Figs. 3-5 (n=12). **c**, Decrease in R_i over development. **d**, R_s of recordings was consistent across ages. Error bars, s.e.m.



Supplementary Figure 6. Short-term exposure to white noise does not balance excitation and inhibition. **a**, Long-term synaptic enhancement across several frequencies after repetitive stimulation with white noise bursts in young AI. Whole-cell recording from AI neuron of a young (P19) rat. First, frequency tuning curves were recorded for 10 minutes (“pre”, gray dashed line) by playing a pseudo-random sequence of pure tones.

Next, 50 ms noise bursts were consistently presented at 0.5 Hz for five minutes. Finally, the pseudo-random sequence was resumed and frequency tuning was recorded for an additional 10+ minutes (“post”, black solid line). Before noise burst stimulation, excitation and inhibition were moderately correlated (r_{pre} : 0.44); after stimulation, the correlation was slightly decreased (r_{post} : 0.28) although overall synaptic strength was increased. Top, excitatory frequency tuning. Excitation across frequencies increased by 25.8% after noise burst stimulation. Bottom, inhibitory frequency tuning. Inhibition across frequencies increased by 20.7% after noise burst stimulation. **b**, Continual white noise also did not balance excitation and inhibition. Whole-cell recording at P18; white noise was continually presented for five minutes after initially measuring synaptic frequency tuning curves. Correlation between excitation and inhibition was unaffected by continual white noise (before white noise, r_{pre} : 0.60; after white noise, r_{post} : 0.67). Top, excitatory frequency tuning. Excitation across frequencies decreased by -16.3% after five minutes of continual white noise. Bottom, inhibitory frequency tuning. Inhibition across frequencies decreased by -34.3% after continual white noise. **c**, Summary of changes to synaptic strength and excitatory-inhibitory balance after repetitive noise burst stimulation. In general, excitation and inhibition were both enhanced for many frequencies, but excitatory-inhibitory balance was unchanged. Left, changes to excitation averaged across all frequencies (‘exc’, increase of $91.3 \pm 35.4\%$, $n=12$, $p<0.03$) and inhibition over all frequencies (‘inh’, increase of $44.3 \pm 20.0\%$, $p<0.05$). Right, change in excitatory-inhibitory correlation (decrease of $-0.15 \pm 0.17\%$, $n=12$, $p>0.3$). **d**, Summary of changes to synaptic strength and excitatory-inhibitory balance after continual white noise stimulation. In general, there was no consistent effect on synaptic strength after five

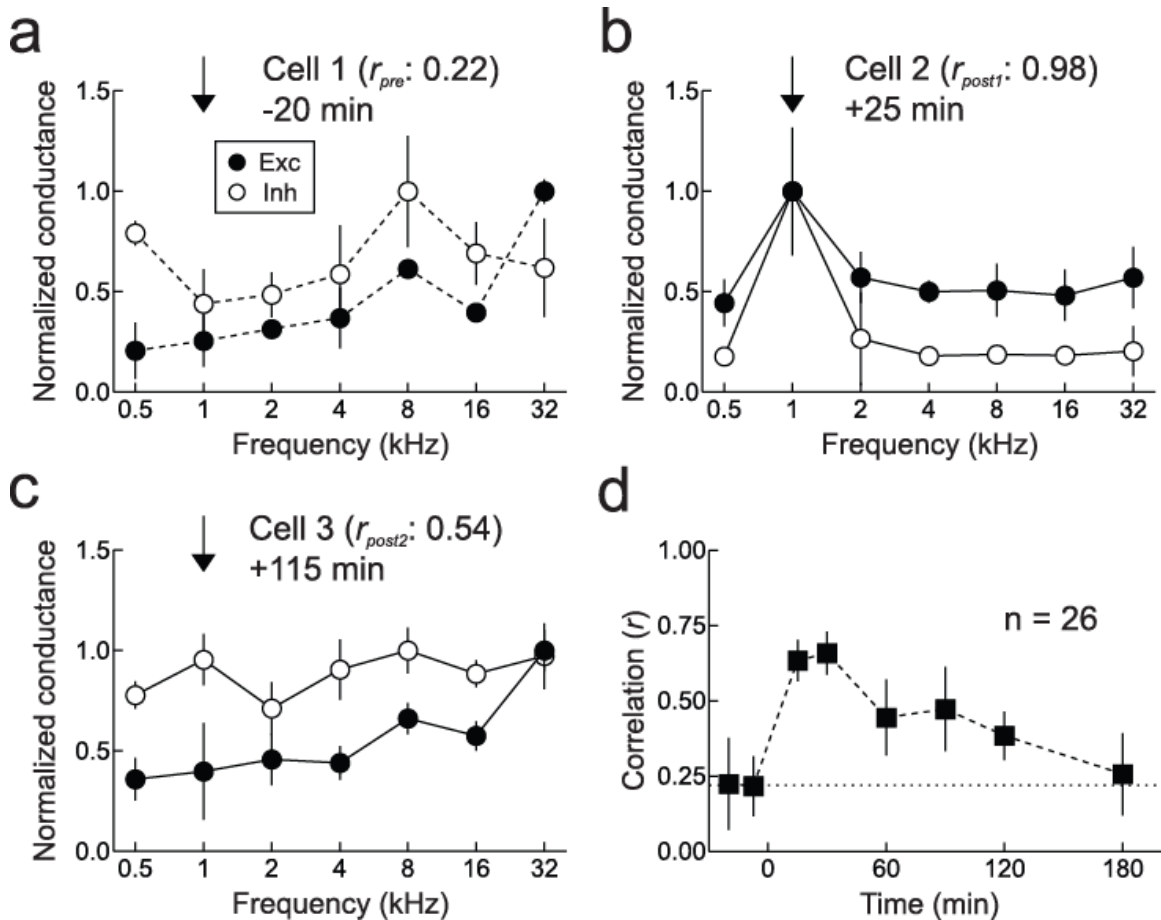
minutes of continual white noise, and excitatory-inhibitory balance was unaffected. Left, changes to excitation averaged across all frequencies ('exc', increase of $10.4 \pm 25.9\%$, $n=5$, $p>0.7$) and inhibition over all frequencies ('inh', increase of $9.0 \pm 27.6\%$, $p>0.7$). Right, change in excitatory-inhibitory correlation (decrease of $-0.04 \pm 0.04\%$, $n=5$, $p>0.3$). Error bars, s.e.m.



Supplementary Figure 7. Development of tone-evoked spike output. **a**, During development, sensory-evoked spiking in AI was temporally imprecise. Shown here are

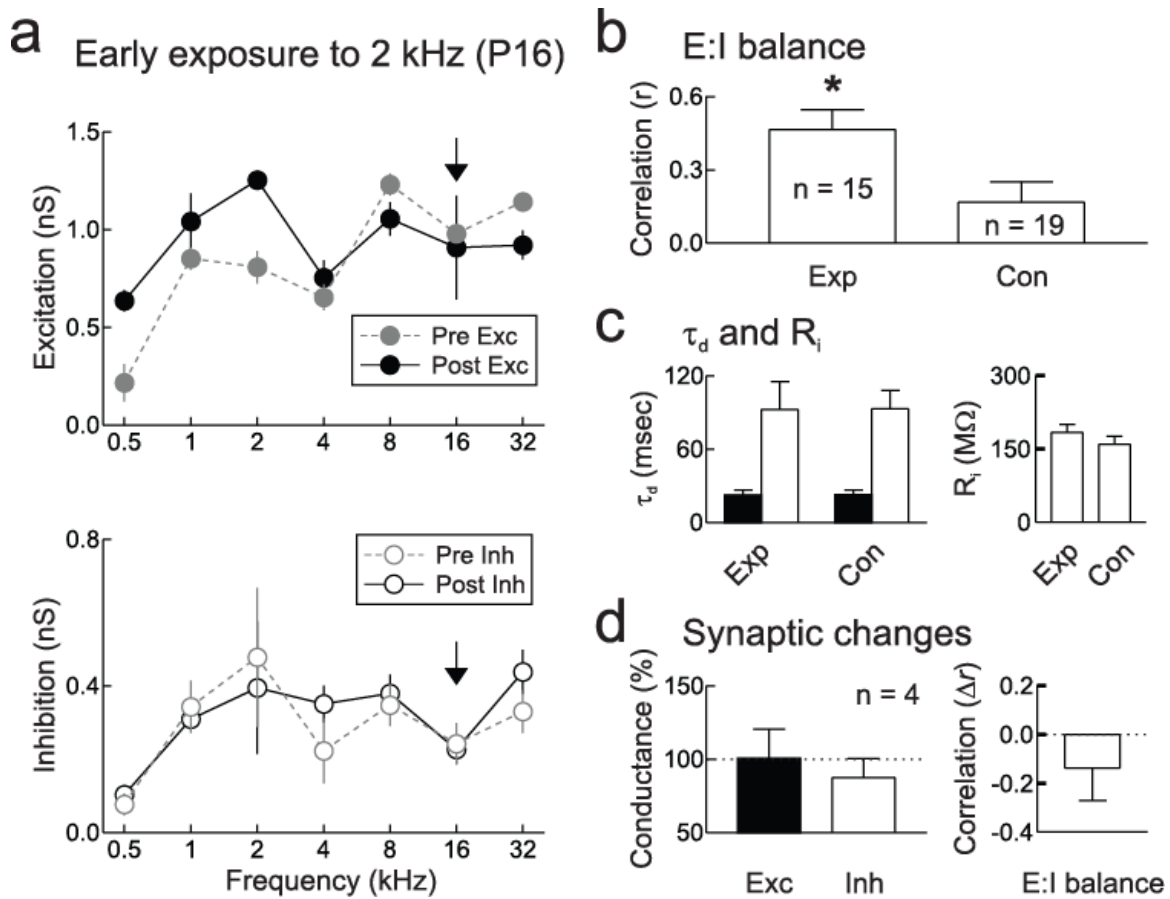
examples of spikes evoked at best frequency during whole-cell current-clamp recording (left, P13 cell) and cell-attached recording (right, P19 cell). Temporal precision of spiking was quantified as the standard deviation of the latency to the first tone-evoked spike ('jitter', σ : 34.0 ± 8.4 msec, $n=9$; mean age: $P16 \pm 1$). Some experiments (3/9 cells) were performed in cell-attached mode to ensure that whole-cell recording methods did not greatly affect spiking. **b**, Spike firing was temporally precise in adult AI. Spikes evoked at best frequency are shown for whole-cell current clamp recording (left) and cell-attached recording (right) from two different cells. Note difference in scale bar from subpanel a. Spike jitter was significantly lower in adults than in young animals (σ : 8.8 ± 2.1 msec, $n=13$, $p < 0.01$ compared to young neurons, 2/13 cells recorded in cell-attached mode). **c**, Patterned stimulation changes spiking frequency tuning curves in young animals. Example whole-cell current-clamp recording of a P13 cell with original best frequency of 32 kHz. After measuring the spiking tuning curve (grey dashed line), 8 kHz tones were repetitively presented for 3 minutes. Afterward (solid black line), responses at 8 kHz were greatly increased (before: 0.13 ± 0.09 spikes/trial, after: 0.51 ± 0.09 spikes/trial, enhancement of 392.3%, $p < 0.005$); enhancements also spread to neighboring frequencies, while responses to the original best frequency were suppressed (responses to 32 kHz before: 0.94 ± 0.11 spikes/trial, after: 0.53 ± 0.09 spikes/trial, decrease of -43.6% , $p < 0.01$), likely as a consequence of similar sets of changes to synaptic inputs shown in Figs. 3 and 4. **d**, Patterned stimulation did not affect spiking tuning curves in adult AI. Example of an adult AI neuron in which repetitive presentation of 16 kHz tones did not enhance spike output (before: 0.44 ± 0.18 spikes/trial, after: 0.35 ± 0.11 spikes/trial, decrease of -20.5% , $p > 0.6$). **e**, Summary of experimentally-measured effects of patterned

stimulation on spike output at the presented frequency (left; young: spikes/trial increase of $204.8 \pm 53.4\%$, $n=5$, $p<0.05$; adult: increase of $6.3 \pm 10.4\%$, $n=6$, $p>0.5$) and temporal precision (right; young: jitter decrease of $-50.2 \pm 13.7\%$, $n=5$, $p<0.01$; adult: increase of $5.0 \pm 23.9\%$, $n=6$, $p>0.5$). **f**, Summary of computer simulations using a conductance-based integrate and fire neuron with parameters of synaptic conductance, jitter, and threshold taken from experiments (see Methods). Simulations were run 50 times in each case (before and after simulating the effects of patterned stimulation), and correctly predicted the increase in spiking and decrease in jitter for young neurons (spikes/trial increase of 163.2% , temporal jitter decrease of -41.8% , $p<0.05$ compared to adults) and the lack of effect for adult neurons (spikes/trial increase of 9.1% ; temporal jitter increase of 4.5%). Error bars, s.e.m.



Supplementary Figure 8. Temporal dynamics of developmental excitatory-inhibitory balancing by a brief episode of patterned stimulation. **a**, Normalized frequency tuning of synaptic excitation (filled) and inhibition (open) for the first cell 20 minutes prior to four minutes of patterned stimulation with 1 kHz tones. Synaptic conductances were normalized to the amplitude of the largest amount of excitation and inhibition across frequencies. The excitation-inhibition correlation was initially low ($r_{pre}: 0.22$). Arrow indicates the presented frequency (1 kHz). **b**, Normalized frequency tuning of a second cell from the same animal 25 minutes after the end of patterned stimulation. The excitatory-inhibitory correlation is much higher ($r_{post1}: 0.98$), due to the enhancement of excitation and inhibition at the presented frequency. **c**, Third cell from the same animal,

recorded 115 minutes after patterned stimulation. The correlation between excitation and inhibition has begun to weaken (r_{post2} : 0.54), possibly due to lack of consolidation by further patterned stimulation, or extinction by continual exposure to the pseudo-random tone sequence used to measure synaptic tuning curves. **d**, Time course for enhancement of excitatory-inhibitory balancing (n=2-15 at each time point, for a total of 56 measurements from 26 different neurons in 15 different animals). Time is relative to the end of the patterned stimulation procedure. Error bars, s.e.m.



Supplementary Figure 9. Early exposure to pure tonal stimuli accelerates cortical synaptic receptive field development to precociously close the critical period. Rat pups were continually exposed in their home cages to either 2 kHz tones or 7 kHz tones starting from P9-P11 for one to three days. **a**, Whole-cell recording of a P16 cell from an animal exposed to 2 kHz tones between P11-P14. Excitatory-inhibitory correlation was high (r_{pre} : 0.66). After initially measuring these synaptic tuning curves (gray dashed lines), 16 kHz tones were repetitively presented for five minutes. This period of patterned stimulation had no significant effect on tuning curves measured ten minutes later (solid black lines) in terms of either excitatory-inhibitory balance (r_{post} : 0.64) or absolute synaptic strength at the presented frequency (change in 16 kHz-evoked excitation from

0.98 nS to 0.91 nS or -9.1% , $p>0.7$; change in inhibition from 0.24 nS to 0.23 nS or -4.2% , $p>0.8$). **b**, Average correlation of excitation and inhibition for animals exposed to repetitive tonal stimuli early in life ('exp', $n=15$; age: 14.3 ± 0.3 days; $r: 0.47\pm 0.08$) was much higher than the average correlation of age-matched controls ('con', $n=19$; age: 13.9 ± 0.3 days, $p>0.3$ compared to early exposed animals; $r: 0.17\pm 0.08$, $p<0.02$). **c**, Synaptic decay kinetics (τ_d) and input resistance (R_i) were similar (τ_d , $p>0.9$ for excitation and inhibition; R_i , $p>0.3$) between animals exposed to tones early in life and animals raised under normal laboratory conditions. **d**, Synaptic responses and excitatory-inhibitory balance were unaffected by a few minutes of patterned stimulation during whole-cell recording, in animals exposed to tones early in life (change in excitation at presented frequency: $0.9\pm 19.9\%$, $n=4$, $p>0.9$; change in inhibition at presented frequency: $-12.4\pm 13.1\%$, $p>0.4$; change in excitatory-inhibitory correlation across frequencies: -0.14 ± 0.13 , $p>0.3$). Error bars, s.e.m.